

This article was downloaded by:

On: 16 January 2011

Access details: *Access Details: Free Access*

Publisher *Taylor & Francis*

Informa Ltd Registered in England and Wales Registered Number: 1072954 Registered office: Mortimer House, 37-41 Mortimer Street, London W1T 3JH, UK



Journal of Energetic Materials

Publication details, including instructions for authors and subscription information:

<http://www.informaworld.com/smpp/title~content=t713770432>

Three-dimensional modeling of explosive desensitization by preshocking by

Charles L. Mader^a; James D. Kershner^a

^a Los Alamos National Laboratory, Los Alamos, New Mexico, USA

To cite this Article Mader, Charles L. and Kershner, James D.(1985) 'Three-dimensional modeling of explosive desensitization by preshocking by', *Journal of Energetic Materials*, 3: 1, 35 – 55

To link to this Article: DOI: 10.1080/07370658508221234

URL: <http://dx.doi.org/10.1080/07370658508221234>

PLEASE SCROLL DOWN FOR ARTICLE

Full terms and conditions of use: <http://www.informaworld.com/terms-and-conditions-of-access.pdf>

This article may be used for research, teaching and private study purposes. Any substantial or systematic reproduction, re-distribution, re-selling, loan or sub-licensing, systematic supply or distribution in any form to anyone is expressly forbidden.

The publisher does not give any warranty express or implied or make any representation that the contents will be complete or accurate or up to date. The accuracy of any instructions, formulae and drug doses should be independently verified with primary sources. The publisher shall not be liable for any loss, actions, claims, proceedings, demand or costs or damages whatsoever or howsoever caused arising directly or indirectly in connection with or arising out of the use of this material.

THREE-DIMENSIONAL MODELING OF EXPLOSIVE DESENSITIZATION BY PRESHOCKING

by

Charles L. Mader and James D. Kershner
Los Alamos National Laboratory
Los Alamos, New Mexico 87545 (USA)

ABSTRACT

The reactive three-dimensional hydrodynamic Code 3DE has been used to investigate the reactive hydrodynamics of desensitization of heterogeneous explosives by shocks too weak to initiate propagating detonation in the geometries studied.

The preshock desensitizes the heterogeneous explosive by closing the voids and making it more homogeneous. A higher pressure second shock has a lower temperature in the multiple shocked explosive than in single shocked explosive. The multiple shock temperature may be low enough to cause a detonation wave to fail to propagate through the preshocked explosive.

Journal of Energetic Materials vol. 3, 35-55 (1985)
This paper is not subject to U.S. copyright.
Published in 1985 by Dowden, Brodman & Devine, Inc.

INTRODUCTION

Shock initiation of heterogeneous explosives proceeds by the process of shock interaction at density discontinuities such as voids which produces local hot spots that decompose and add their energy to the flow. The released energy strengthens the shock so that when it interacts with additional inhomogeneities, higher temperature hot spots are formed and more of the explosive is decomposed. The shock wave grows stronger and stronger, releasing more and more energy until propagating detonation occurs. The process has been numerically modeled using the technique called Forest Fire.¹ It describes the decomposition rates as a function of the Pop plot (the experimentally measured distance of run to detonation as a function of the shock pressure) and the reactive and nonreactive Hugoniot.

It has been observed that preshocking a heterogeneous explosive with a shock pressure too low to cause propagating detonation in the time of interest can cause a propagating detonation in unshocked explosive to fail to continue propagating when the detonation front arrives at the previously shocked explosive. The resulting explosive desensitization was modeled using a Forest Fire decomposition rate that was determined only by the initial shock pressure of the first shock wave passing through the explosive.² This model could reproduce the experimentally observed explosive desensitization of TATB (triamino-trinitrobenzene) explosives previously shocked by short duration 25 and 50-kilobar pulses. It could not reproduce the observed results for low or high preshock pressures that do not cause a propagating detonation to fail.

The purpose of this study was to determine the mechanism of the explosive desensitization by preshocking using a three-dimensional reactive hydrodynamic model of the process. With the mechanism determined, it was possible to modify the decomposition rate to include both the desensitization and failure to desensitize effects.

Experimental Studies

Dick³ performed a PHERMEX radiographic study of detonation waves in PBX-9502 (95/5 Triaminotrinitrobenzene/Kel-F binder at 1.894 g/cm^3) proceeding up a 6.5- by 15.0-cm block of explosive that was preshocked by a 0.635-cm steel plate moving at 0.08 (Shot 1698) or 0.046 cm/ μs (Shot 1914). The static and dynamic radiograph for Shot 1698 are shown in Fig. 1. The preshocked PBX-9502 explosive quenches the detonation wave as it propagates into the block of explosive.

Travis and Campbell⁴ performed a series of experiments studying desensitization of PBX-9404 (94/3/3 HMX/Nitrocellulose/CEF at 1.844 gm/cm^3) by shocks. The PBX-9404 explosive was 8 x 4 x 1/3 in. and cemented to a thick sheet of Plexiglas. It was immersed in water at various distances from a 6-in.-diameter sphere of PBX-9205 which served as the preshock generator. When the arrangement was fired, a detonation swept downward through the PBX-9404 and encountered an upward-spreading shock wave from the PBX-9205 generator. Events were photographed with a framing camera.

They concluded that the detonation in PBX-9404 is not quenched by a preshock of 7.5 kbars. An 11-kbar initial shock pressure required a time lapse of about 6 μs before the detonation wave failed and a 25-kbar preshock required less than 1 μs .

THREE-DIMENSIONAL MODELING

To investigate the mechanism of explosive desensitization by preshocking, we used the reactive hydrodynamic code called 3DE.⁵ It uses numerical techniques identical to those described in detail in Reference 1. It has been used to study the interaction of multiple detonation waves,⁶ the basic processes in shock initiation of heterogeneous explosives,^{7,8} and the reactive hydrodynamics of a matrix of tungsten particles in HMX.⁹

The HOM equation-of-state constants for TATB, which consist of the BKW detonation product and the solid equation-of-state constants, are given in Reference 7. The Arrhenius reactive rate law was used for TATB with the constants determined for solid TATB by Raymond N. Rogers¹ of an activation energy of 59.9 kcal/mole and a frequency factor of $3.18 \times 10^{13} \mu\text{s}^{-1}$.

A constant velocity piston was applied to the bottom of a TATB explosive cube shocking the explosive to the desired pressure. When a higher pressure second shock was to be introduced, the piston velocity was increased and other piston state values changed as appropriate for a multiple shock of the required pressure.

A single shock pressure of 290 kbars in TATB has a density of 2.8388 g/cm³, particle velocity of 0.21798 cm/ μs , energy of 0.02376 mb cc/g, and temperature of 1396 °K. A second shock pressure of 290 kbars in TATB initially shocked to 40 kbars has a density of 2.878 g/cm³, energy of 0.017759 mb-cc/g, particle velocity of 0.2040 cm/ μs , and temperature of 804.2 °K.

When a shock wave interacts with a hole, a hot spot with temperatures hotter than the surrounding explosive is formed in the region

above the hole after it is collapsed by the shock wave. The hot region decomposes and contributes energy to the shock wave, which has been degraded by the hole interaction.

Whether this energy is sufficient to compensate for the loss from the hole interaction depends upon the magnitude of the initial shock wave, the hole size, and the interaction with the flow from nearest neighbor hot spots.

The hole size present in pressed explosives varies from holes of 20 to 600 Å in the TATB crystals to holes as large as 0.05 cm in the explosive-binder matrix. Most of the holes vary in size from 0.005 to 0.0005 cm in diameter, so we examined holes in that range of diameters.

The interaction of a 40-kbar shock with a single 0.004-cm-diameter air hole in TATB was modeled. The three-dimensional computational grid contained 15 by 15 by 36 cells each 0.001 cm on a side. The time step was 0.0002 μs. After 0.025 μs, the 40-kbar shock had collapsed the hole and a 290-kbar shock wave was introduced which passed through the 40-kbar preshocked region and overtook the 40-kbar shock wave.

The shock temperature in the bulk of the TATB and the adiabatic explosion times are given below:

First Shock (kbar)	40	290	40
Second Shock (kbar)			290
Temperature (°K)	362.5	1396	804.2
Explosion Time (μs)	10^{19}	10^{-6}	3.85

Thus, the multiple shocked explosive would require 3.85 μs for a propagating detonation to form and only 10^{-6} μs if singly shocked to 290 kbar.

The density and burn fraction surface contours are shown in Figs. 2 and 3 and the cross sections through the center of the hole are shown in Fig. 4.

The 40-kbar shock wave collapsed the hole and formed a small weak hot spot which was not hot enough to result in appreciable decomposition of the TATB.

The 290-kbar shock wave temperature was not hot enough to cause explosion during the time studied in the bulk of the explosive previously shocked to 40 kbars; however, the additional heat present in the hot spot formed by the 40-kbar shock wave after it interacted with the hole was sufficient to decompose some of the explosive after it was shocked by the 290-kbar wave.

Propagating detonation occurred immediately after the 290-kbar shock wave caught up with the 40-kbar preshock.

To investigate the effect of the interaction of a matrix of holes with a multiple shock profile, a matrix of 10% air holes located on a hexagonal close packed lattice in TATB was modeled. The spherical air holes had a diameter of 0.004 cm. The initial configuration is shown in Fig. 5. The three-dimensional computational grid contained 16 by 22 by 36 cells each 0.001 cm on a side. The time step was 0.0002 μ s. Figure 6 shows the density and mass fraction cross sections for a 40-kbar shock wave followed after 0.045 μ s by a 290-kbar shock wave interacting with a matrix of 10% air holes of 0.004-cm-diameter in TATB.

The preshock desensitized the explosive by closing the voids and made it more homogeneous. The higher pressure second shock wave proceeded through the preshocked explosive until it caught up with the preshock.

The three-dimensional modeling study demonstrated that the desensitization occurs by the preshock interacting with the holes and eliminating the density discontinuities. The subsequent higher pressure shock waves interact with a more homogeneous explosive. The multiple shock temperature is lower than the single shock temperature at the same pressure, which is the cause of the observed failure of a detonation wave to propagate in preshocked explosives for some ranges of preshock pressure.

The modification indicated by the three-dimensional study to the Forest Fire decomposition rate being limited by the initial shock pressure was to add the Arrhenius rate law to the Forest Fire rate.

The Forest Fire rate for TATB is shown in Fig. 7 along with the Arrhenius rate calculated using the temperatures from the HOM equation-of-state for the partially burned TATB associated with the pressure as determined by Forest Fire. We will proceed using a burn rate determined by Forest Fire limited to the initial shock pressure and the Arrhenius rate using local partially burned explosive temperatures.

TWO-DIMENSIONAL MODELING

The experimental geometries studied using PHERMEX shown in Fig. 1 were numerically modeled using a reactive hydrodynamic computer code, 2DL, that solves the Navier-Stokes equation by the finite-difference techniques described in Reference 1. The users manual for the 2DL code is described in Reference 10. For explosives that have been previously shocked, Craig⁵ experimentally observed that the distance of run to detonation for several multiple shocked explosives was determined primarily by the distance after a second shock had overtaken the lower

pressure shock wave (the preshock). To approximate this experimental observation, we programmed the calculation to use Forest Fire rates determined by the first shock wave or the rates determined by any subsequent release waves that result in lower pressures and lower decomposition rates. As suggested by the three-dimensional study, we added the Arrhenius rate using the local partially burned explosive temperatures to the Forest Fire rate. The HOM equation-of-state and Forest Fire constants used to describe PBX-9502 (X0290) and PBX-9404 are given in Reference 1.

The calculated pressure and mass fraction contours for PHERMEX Shot 1698 are shown in Fig. 8 along with the radiographic interfaces.

The 2DL calculation had 50 by 33 cells to describe the PBX-9502 and 50 by 5 cells to describe the steel plate. The mesh size was 0.2 cm and the time step was 0.04 μs .

The PHERMEX shot was numerically modeled using various velocity steel plates. The results are shown in Table I. The results agree with the experimental evidence that detonation wave failure occurs in preshocked TATB shocked by steel plates with velocities of 0.046 and 0.08 $\text{cm}/\mu\text{s}$.

TABLE I. 9502 Desensitization Calculations

Steel Plate Velocity (cm/ μ s)	Preshock Pressure (kbar)	Result Upon Arrival of Detonation Wave
0.020	9	Detonates preshocked HE
0.030	14	Fails in preshocked HE
0.045	23	Fails in preshocked HE
0.080	50	Fails in preshocked HE
0.100	70	Fails in preshocked HE
0.120	90	Detonates preshocked HE and after 1.5 cm run
0.160	130	Detonates preshocked HE
0.200	180	Detonates preshocked HE

The Travis and Campbell experiments described previously can be evaluated using calculated multiple shock temperatures and solid HMX Arrhenius constants determined from Craig's single crystal shock initiation data.¹¹ His data and the Walsh and Christian¹ shock huginiot temperatures for HMX⁷ are given below:

Pressure (kbars)	Induction Time (μ s)	Calculated Shock Temperature ($^{\circ}$ K)
420	0.05	1809.6
358	0.272	1489.3
320	Failed	1340.0

Using the adiabatic explosion time expression (page 145 of Reference 1)

$$t_{\text{exp}} = \frac{CRT^2}{QZE} e^{E/RT}$$

with $R = 1.987$, $C = 0.4$, and $Q = 800$, we can calculate that the E (activation energy) is 34.8 kcal/mole and Z (frequency factor) is $3.0 \times 10^4 \mu\text{sec}^{-1}$. This is much slower than the liquid HMX constants¹ of

Raymond A. Rogers where $E = 52.7$ kcal/mole and $Z = 5.0 \times 10^{13} \mu\text{sec}^{-1}$.

The solid kinetics of HMX is very complicated with an initial slow reaction succeeded by acceleratory and deceleratory periods. The initial slow reaction has been studied by Maksimov.¹² He reported an activation energy of 37.9 kcal/mole and a frequency factor of $1.58 \times 10^5 \mu\text{sec}^{-1}$. R. Rogers and J. Janney have reported many solid HMX rate constants depending upon where they are studying the reaction period. An unpublished experimental study of the "initial" rate gave an activation energy of 33.9 kcal/mole and a frequency factor of $4.8 \times 10^5 \mu\text{sec}^{-1}$.

The results are summarized below:

<u>Source</u>	<u>E</u>	<u>Z</u>
Craig Shock Initiation Data	34.8	3.0×10^4
Maksimov (initial solid)	37.9	1.6×10^5
Rogers and Janney (initial solid)	33.9	4.8×10^5
Rogers (liquid)	52.7	5.0×10^{13}

Within the experimental errors and the uncertainty associated with the calculated Hugoniot temperatures, the initial solid constants agree with the constants derived from the shock initiation data. The liquid constants are clearly not appropriate for the single crystal HMX shock initiation experiment or for shock desensitization studies.

The calculated 9404 multiple shock results using solid HMX Arrhenius constants obtained from Craig's single crystal shock initiation data are shown in Table II. Induction times less than 0.2 μs were calculated for the 7-kbar preshock that was observed to fail to quench a detonation wave. Induction times of 0.35 to 4 μs were calculated for

the preshock pressures observed to have a time lapse before the detonation wave failed. Larger induction times were calculated for a 50-kbar preshock pressure; however, the 50-kbar pre-shock would build to detonation in 0.4 cm or 0.75 μ s.

The experimental observations of Travis and Campbell are consistent with the desensitization being caused by the preshock making the explosive more homogeneous and reducing the explosive temperature upon arrival of the detonation wave by the multiple shock process.

TABLE II. 9404 Multiple Shock Results

First Shock (kbar)	Second Shock (kbar)	Temperature ($^{\circ}$ K)	Induction Time* (μ s)
360	0	1669	0.051
7	360	1442	0.198
10	360	1368	0.345
15	360	1267	0.821
20	360	1185.1	1.87
25	360	1117.9	4.04
50	360	916.8	84.4

*Solid HMX, $E = 34.5$ kcal/g, $Z = 4.0 \times 10^4 \mu\text{s}^{-1}$

CONCLUSIONS

The desensitization of heterogeneous explosive by preshocking may be attributed to the preshock closing the voids, thus making the explosive more homogeneous. The failure of a detonation wave to propagate in the preshocked explosive may be attributed to the lower temperature that occurs in the multiple shocked explosive than in the singly shocked explosive.

A rate law that combines the Forest Fire rate limited to the rate determined by the initial shock pressure and the Arrhenius rate law permits a description of multiple shocked explosive behavior for many engineering purposes.

REFERENCES

1. Charles L. Mader, Numerical Modeling of Detonations, University of California Press, Berkeley, 1979.
2. Charles L. Mader, Richard D. Dick, "Explosive Desensitization by Preshocking," *Internationale Jahrestagung*, 1979, *Combustion and Detonation Processes*, pp. 569-579 (1979).
3. Charles L. Mader, *LASL PHERMEX Data, Volume III*, University of California Press, Berkeley, 1980.
4. James R. Travis and Arthur W. Campbell, "Explosive Shock Desensitization," accepted for publication in *Eighth Symposium (International) on Detonation* (1985).
5. Charles L. Mader and James D. Kershner, "Three-Dimensional Modeling of Triple-Wave Initiation of Insensitive Explosives," *Los Alamos Scientific Laboratory Report LA-8206* (1980).
6. Charles L. Mader, "Detonation Wave Interactions," *Seventh Symposium (International) on Detonation*, NSWC MP82-334, pp. 669-677 (1981).
7. Charles L. Mader and James D. Kershner, "The Three-Dimensional Hydrodynamic Hot Spot Model Applied to PETN, HMX, TATB, and NQ," *Los Alamos National Laboratory Report LA-10203-MS* (1984).

8. Charles L. Mader and James D. Kershner, "Three-Dimensional Modeling of Shock Initiation of Heterogeneous Explosives," Nineteenth Symposium (International) on Combustion, pp. 685-690 (1982).
9. Charles L. Mader, James D. Kershner, and George H. Pimbley, "Three-Dimensional Modeling of Inert Metal-Loaded Explosives," *Journal of Energetic Materials* 1, 293-324 (1983).
10. James N. Johnson, Charles L. Mader, and Milton S. Shaw, "2DL: A Lagrangian Two-Dimensional Finite-Difference Code for Reactive Media," Los Alamos National Laboratory Report LA-8922 M (1981).
11. Bobby G. Craig, private communication.
12. I. I. Maksimov, *Khimiko-Tekhnologicheskogo Instituta imeni D. I. Mendeleeva*, TRUDY No. 53, pp. 73-84 (1967).

This paper was developed under the auspices of the U.S. Department of Energy.

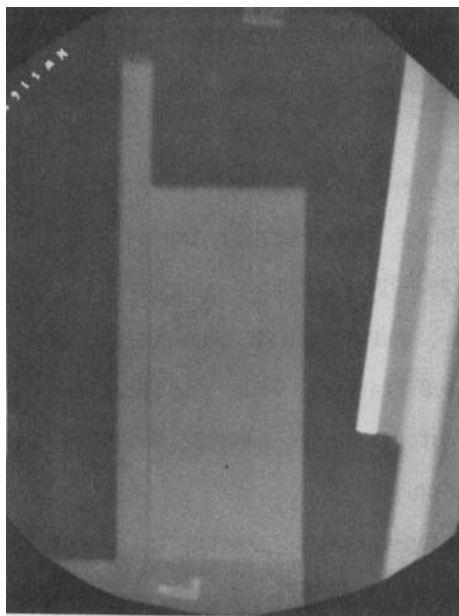


FIGURE 1

Static and dynamic radiograph 1698 of PBX-9502 shocked by a 0.635-cm-thick steel plate going $0.08 \text{ cm}/\mu\text{s}$ and initiated by 2.54 cm of TNT and a P-40 lens.

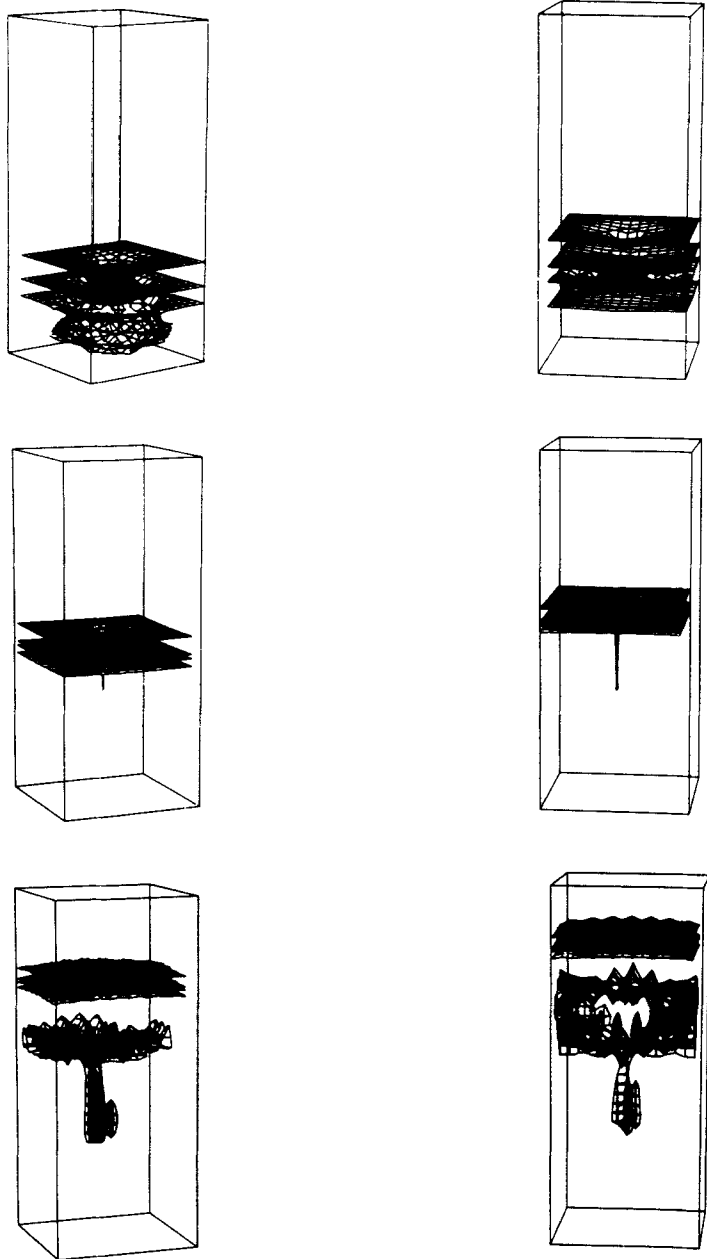


FIGURE 2

The density surface contours for a 40-kbar shock interacting with a single 0.004-cm-diameter air hole in TATB followed after 0.025 μ s by a 290-kbar shock wave.

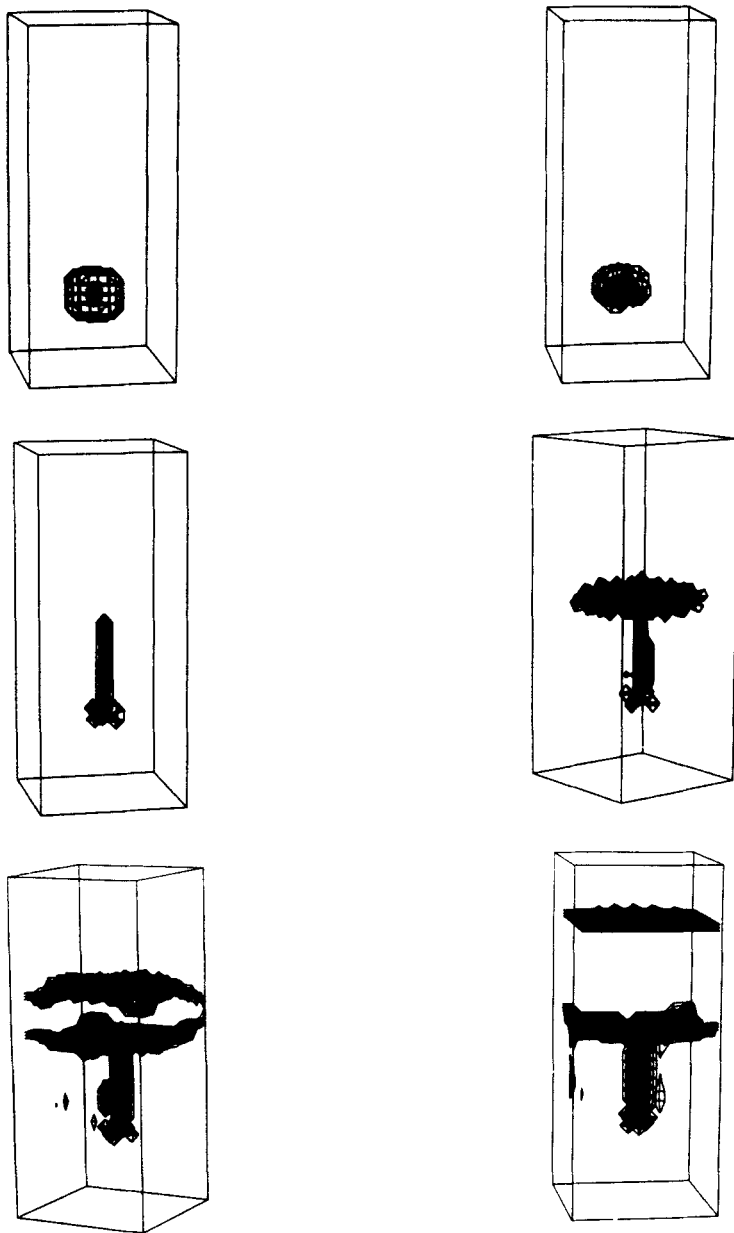


FIGURE 3
The burn fraction contours for the system shown in Fig. 2.

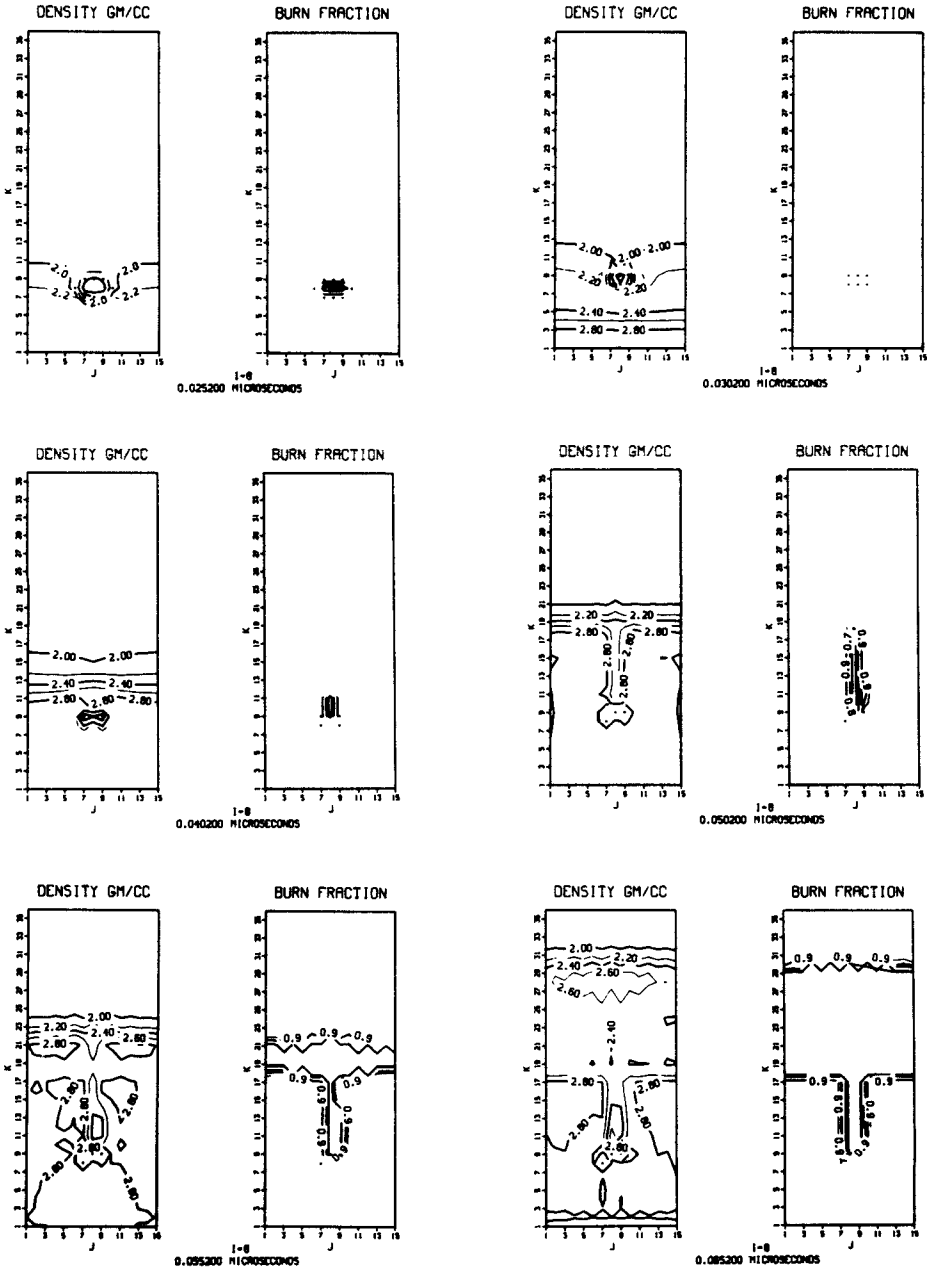


FIGURE 4
 The density and burn fraction cross sections through the center of the hole for the system shown in Fig. 2.

Downloaded At: 14:10 16 January 2011

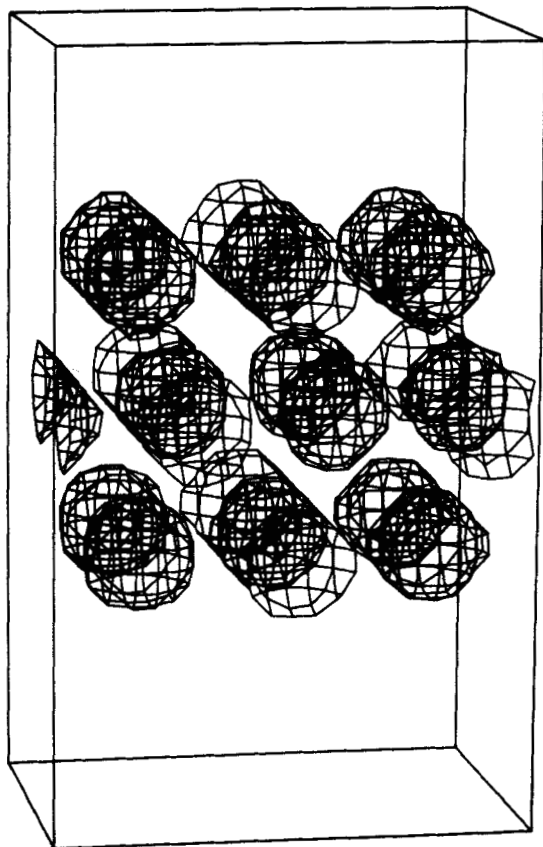


FIGURE 5
The initial configuration of a matrix of 10% air holes in TATB.

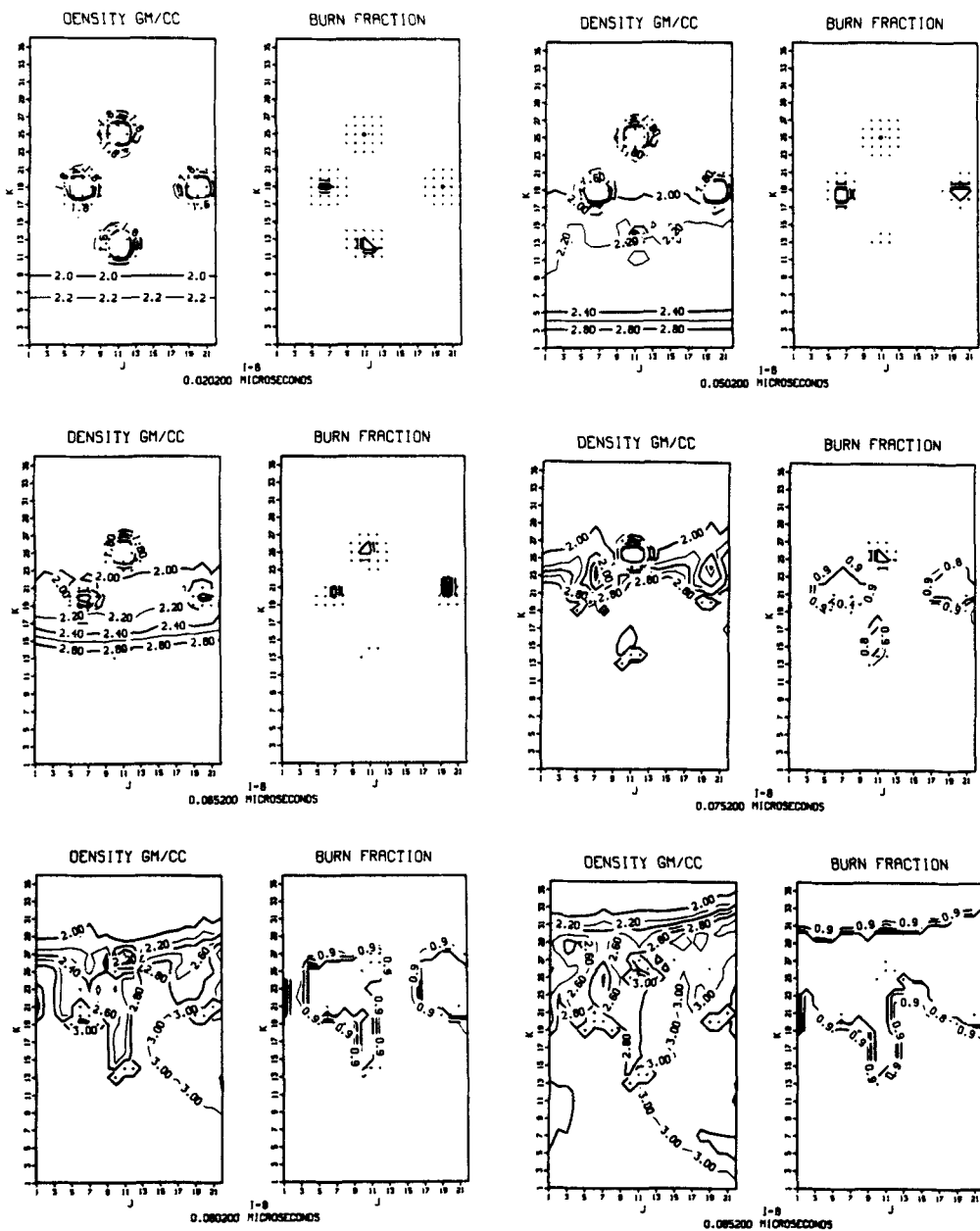


FIGURE 6

The density and mass fractions cross sections are shown for a 40-kbar shock wave followed after 0.045 μ s by a 290-kbar shock wave interacting with a matrix of 10% air holes of 0.004-cm-diameter in ATB.

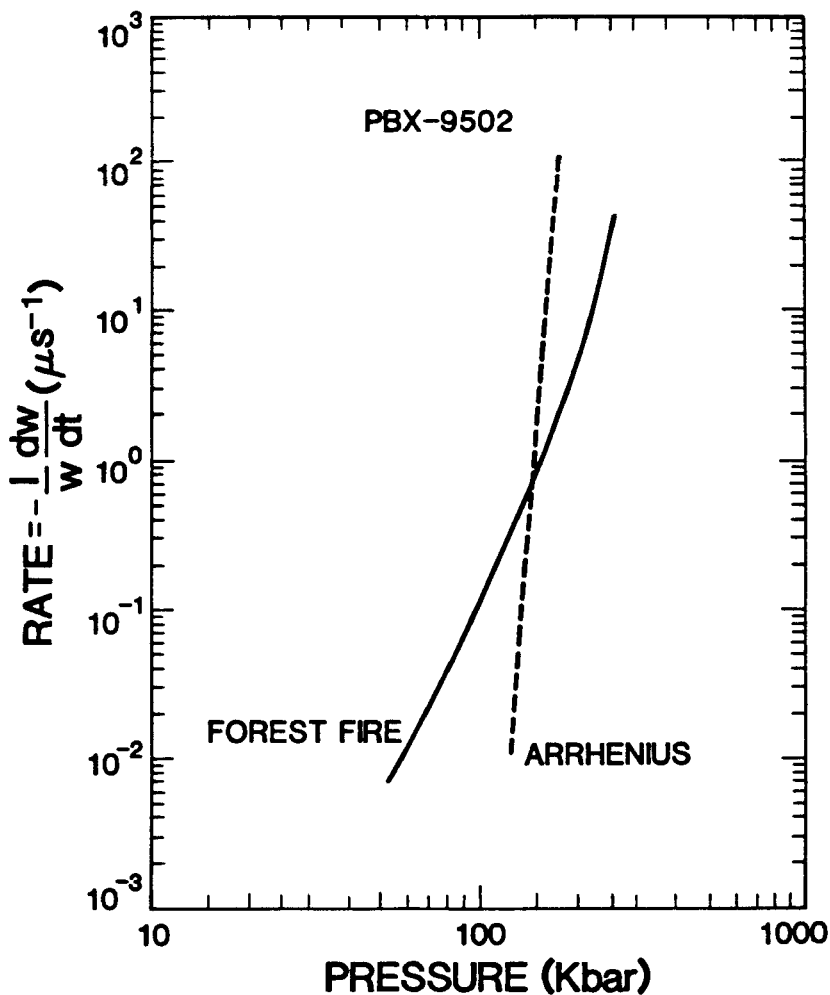


FIGURE 7

The burn rate as a function of pressure for the Forest Fire burn model and the Arrhenius rate law using the HOM temperatures associated with the Forest Fire pressures.

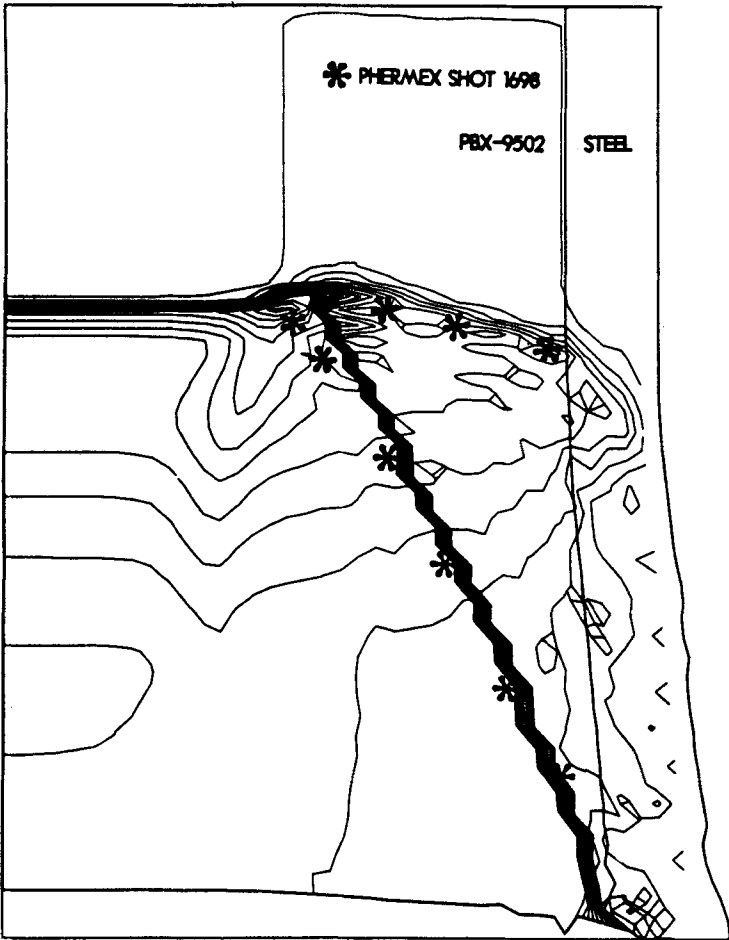


FIGURE 8

The pressure and mass fraction contours for a detonation wave in PBX-9502 interacting with explosive that had been previously shocked to 50 kbars. The PHERMEX radiographic interfaces are shown. The mass fraction contour interval is 0.1 and shown as a thick almost solid line. The pressure contour interval is 40 kbars.